



HAL
open science

Comparative analysis of symbiont ratios and gene expression in natural populations of two *Bathymodiolus* mussel species

H. Guezi, Isabelle Boutet, Ann C. Andersen, F. Lallier, Arnaud Tanguy

► **To cite this version:**

H. Guezi, Isabelle Boutet, Ann C. Andersen, F. Lallier, Arnaud Tanguy. Comparative analysis of symbiont ratios and gene expression in natural populations of two *Bathymodiolus* mussel species. *Symbiosis*, 2015, 63 (1), pp.19-29. 10.1007/s13199-014-0284-0 . hal-01109381

HAL Id: hal-01109381

<https://hal.sorbonne-universite.fr/hal-01109381>

Submitted on 26 Jan 2015

HAL is a multi-disciplinary open access archive for the deposit and dissemination of scientific research documents, whether they are published or not. The documents may come from teaching and research institutions in France or abroad, or from public or private research centers.

L'archive ouverte pluridisciplinaire **HAL**, est destinée au dépôt et à la diffusion de documents scientifiques de niveau recherche, publiés ou non, émanant des établissements d'enseignement et de recherche français ou étrangers, des laboratoires publics ou privés.

27 **Abstract**

1
2
3 28 *Bathymodiolus* mussels associated with deep-sea hydrothermal vents and cold seeps harbor
4 29 chemosynthetic endosymbiotic bacteria in bacteriocytes located in the gill epithelium. Two
5 30 distinct morphotypes of γ -proteobacteria, sulfur- and methane-oxidizing, have been identified
6 31 and form a dual symbiosis in *B. azoricus* mussels from the Mid-Atlantic Ridge and in *B. aff.*
7
8
9 32 *boomerang* from cold seeps in the Gulf of Guinea. Thiotropic bacteria (SOX) are capable of
10 33 fixing CO₂ in the presence of sulfide or thiosulfate and methanotrophic bacteria (MOX) use
11 34 methane both as a carbon and an energy source. In this study we used quantitative real-time
12 35 PCR to test whether symbiont abundance and gene expression varied between the two mussel
13 36 species. Results showed that *B. azoricus* from two hydrothermal sites had similar ratios and
14 37 gene expression pattern for both symbiont types. In *B. aff. boomerang*, SOX ratio and ATP
15 38 sulfurylase gene expression show differences between specimens collected on the different
16 39 sites. Analysis of symbiont ratios in both species indicated a clear dominance of MOX
17 40 symbionts in *B. aff. boomerang* and SOX symbionts in *B. azoricus*. We also evidenced that
18 41 the species from the deeper sites (*B. aff. boomerang*) and mussels collected from sulfur and
19 42 methane rich habitats showed higher symbiont ratio suggesting that environmental parameters
20 43 may have significant impacts on the symbiont ratios in *Bathymodiolus* mussels.
21
22
23
24
25
26
27
28
29
30
31
32
33
34
35
36
37
38
39
40
41
42
43
44
45
46
47
48
49
50
51
52
53
54
55
56
57
58
59
60
61
62
63
64
65

47 Keywords: Hydrothermal vent, Cold seeps, *Bathymodiolus*, symbiont, FISH

49 Abbreviations:

50 DAPI: 4',6-DiAmidino-2-Phenyl-Indole, double-stranded DNA staining

51 Cy3 and Cy5: Cyanine dyes

52 FISH: Fluorescent In Situ Hybridization

53 MOX: Methane OXidizing bacteria

54 pmoA: particulate methane oxygenase, subunit A

55 ROV: Remotely Operated Vehicle

56 SOX: Sulfur OXidizing bacteria

61 **1 Introduction**

62 Hydrothermal vents and cold seeps are two unique ecosystems that have been discovered
63 while exploring the deep ocean. Deep-sea hydrothermal vents occur in geologically active
64 regions of the ocean floor. Seawater percolates into the Earth's crust through fissures in the
65 ocean floor where it is heated and modified before the water expands and rises back to the
66 surface (Lonsdale and Becker 1985; Van Dover 2000). As it rises, the hot water dissolves
67 minerals and other chemicals from the surrounding rocks. When it reaches the ocean floor, it
68 mixes with cold deep-sea water, and some of the minerals precipitate out of the seawater and
69 harden on the rim of the vent to form over the time a tall chimney-like structure (Tivey 1995;
70 Von Damm 1995). The temperature of the water coming out of these vents may exceed 360°C
71 and is characterized by a low pH, high levels of hydrogen sulfide, methane and/or hydrogen,
72 high metal concentrations and anoxia (Geret et al. 2002; Charlou et al. 2002; Le Bris et al.
73 2003; German et al. 2004).

74 A few years after the discovery of hydrothermal vents, another environment called cold seeps
75 and associated with mineral-rich water rising through sedimented sea floor was discovered.
76 Cold seeps occur in geologically active and passive continental margins where pore waters
77 enriched in methane are forced upward through the sediments by pressure (Sibuet and Olu
78 1998; Kojima 2002; Levin 2005). Gradient seeps are areas where chemically derived fluids
79 from hydrocarbon reservoirs and methane hydrates arise (Van Dover 2002; Dickens et al.
80 2003; Olu-Le Roy et al. 2007). Both environments share common characteristics such as the
81 presence of reduced chemical compounds (H_2S , CH_4 and other hydrocarbonates), local
82 hypoxia, and abundant metabolically active bacterial populations. Hydrothermal vents and
83 cold seeps also differ in significant ways; hydrothermal vents are characterized by locally
84 high temperatures and strongly fluctuating reduced chemical concentrations associated with
85 various chimney life time (Van Dover and Trask 2000; Vanreusel et al. 2010; German et al.
86 2004), while cold seeps are often assumed to be more stable in time, even when they show
87 heterogeneity in their environmental characteristics (Sibuet and Olu 1998; Boetius and Seuss
88 2004; Vanreusel et al. 2010). Deep-sea hydrothermal vent fields and cold seeps are areas on
89 the seafloor with great biological productivity fueled by microbial chemosynthesis and with
90 substantial animal populations (Van Dover et al. 2003; Levin 2005; MacDonald et al. 1989;
91 Sibuet and Olu 1998). Bathymodioline mussels are dominant constituents of the deep-sea
92 fauna (Kenk and Wilson 1985; Nelson and Fisher 1995; DeChaine and Cavanaugh 2006;

93 Dubilier et al. 2008; Génio et al. 2008). Beside vents and seeps, these mussels colonize
94 various environments such as whale falls and sunken wood showing a great ability to adapt to
95 different habitats (Cavanaugh et al. 2006). One key to the survival of these mussels in such
96 environments is their association with chemosynthetic bacterial symbionts (Sibuet and Olu
97 1998; Van Dover and Trask 2000). All Bathymodiolus species harbor one or several types of
98 symbionts. Some species host only sulfur-oxidizing bacterial symbionts (Nelson et al. 1995;
99 Fujiwara et al. 2000) like *B. thermophilus* (Desbruyeres et al. 2001), which are capable of
100 CO₂ fixation with sulfide or thiosulfate oxidation as an energy source (Cavanaugh 1983;
101 Nelson et al. 1995). Other species, including *B. childressi* host only methanotrophic
102 symbionts which use methane both as a carbon and an energy source (Childress et al. 1986;
103 Barry et al. 2002; Pimenov et al. 2002; DeChaine and Cavanaugh 2006; Fujiwara et al. 2000).
104 Other mussel species such as *B. aff. boomerang* and *B. azoricus* host both types of bacteria
105 (Fisher et al. 1993; Distel et al. 1995; Robinson et al. 1998; Fiala-Médioni et al. 2002).
106 Recently, four symbionts were discovered in *B. heckerae* (Fisher et al. 1993) and, in a small
107 *Idas* mussel, six distinct bacterial 16S rRNA phylotypes were identified (Duperron et al.
108 2008). Previous immunological studies and enzyme assays have confirmed the presence of
109 dual symbionts in both *B. azoricus* and *B. aff. boomerang*. In particular, ATP sulfurylase
110 which indicates the potential for sulfur oxidation, and particulate methane oxygenase (pmoA)
111 which indicates the potential for aerobic methane oxidation (Fisher et al. 1987; Robinson et
112 al. 1998; Pimenov et al. 2002), were both found in the same gill tissue of *B. azoricus* and *B.*
113 *aff. boomerang* (Duperron et al. 2005, Duperron et al. 2007). This dual symbiosis provides the
114 mussels with two distinct sources of energy and carbon, which allows them flexibility and
115 adaptability to their fluctuating environments (Distel et al. 1995). Endosymbiosis of
116 chemoautotrophic bacteria in mussels plays a key-role in the ecology and biogeochemistry of
117 deep-sea hydrothermal vents and cold seeps. Symbionts derive energy by oxidizing reduced
118 compounds (*e.g.*, sulfide, methane, hydrogen), which enable them to fix inorganic carbon
119 providing nutrition to their hosts (Felbeck et al. 1981; Childress et al. 1986, 1991; Guirgis and
120 Childress 2006). The nutritional role of bacteria has been estimated using stable isotope
121 analysis in *B. heckerae* (Van Dover et al. 2003), *B. brooksi* and *B. childressi* (Duperron et al.
122 2007; Olu-Leroy et al. 2007), *B. azoricus* (Riou et al. 2010) and recently in *B. aff. boomerang*
123 (Duperron et al. 2011). The bacteria are transmitted horizontally between mussels and have
124 not yet been cultured outside of their hosts limiting the study of these symbiotic
125 chemosynthetic bacteria (Le Pennec et al. 1988; Won et al. 2003; Salerno et al. 2005; Kàdàr et
126 al. 2005)

127 Several studies have been conducted that link symbiont ratios to the local environment
128 parameters. The relative abundance of each symbiont is influenced by the hydrothermal fluid
129 characteristics, especially methane and sulfide concentrations. Recently, symbiont ratios and
130 metabolic gene expression were shown to vary significantly among specimens of *B. azoricus*
131 from two contrasted hydrothermal vent sites, Menez Gwen and Rainbow. Specimens of *B.*
132 *azoricus* from Rainbow (a hydrothermal site rich in methane) had a high concentration of
133 methane oxidizing (MOX) bacteria and a high level of *pmoA* expression compared to Menez
134 Gwen mussels (a hydrothermal site rich in sulfide), which showed a greater abundance in
135 sulfur-oxidizing (SOX) bacteria and higher level of ATP sulfurylase gene expression (Boutet
136 et al. 2011). In another study, a lower abundance of MOX symbionts was detected in mussels
137 from Lucky Strike compared to Menez Gwen individuals using TEM micrographs analysis
138 (Fiala-Médioni et al. 2002). Using a fluorescence *in situ* hybridization protocol coupled with
139 3-dimensional reconstruction of bacteriocyte sections (3D FISH), Halary et al (2008) also
140 demonstrated that specimens of *B. azoricus* from different aggregates of animals within a
141 single site varied in their symbiont abundances. On the contrary *B. aff. boomerang* collected
142 from different mussel-aggregates within the giant cold seep pockmark REGAB (800m in
143 diameter) showed a relatively homogenous symbiont ratios (Duperron et al. 2011). The two
144 latter studies aimed at understanding the mechanisms developed by endosymbiont bacteria to
145 adapt in response to changing environmental parameters. However, our understanding of the
146 inter- and intra-site variability of the mussel symbiont ratios in contrasting ecosystems is
147 poor. To explore this variability, we compared symbiont ratios and gene expression in two
148 *Bathymodiolus* species from different habitats (vents/seeps), and from different sites within
149 each habitat. We investigated the variability of their relative abundance and the gene
150 expression of both symbionts in the two mussel species using real time PCR and we applied
151 the FISH technique for a visual confirmation of the bacterial dominance in the mussel gills.

153 **2 Material and methods**

154 **2.1 Animal collection**

155 *B. azoricus* individuals were sampled at two vent fields: Menez Gwen (MG: 37°50' N, 31°31'
156 W, 830m depth; n =33), and Lucky Strike (LS: 37°17' N, 32°28' W, 1700m depth; n =22) in
157 the Azores region of the Mid-Atlantic Ridge using the ROV (Remotely Operated Vehicle)
158 Victor 6000 operated from the ship N/O Pourquoi Pas? during the BIOBAZ cruise in July

159 2011. *B. aff. boomerang* specimens were collected at three sampling areas, W01 (n=28), W02
160 (n=43) and NW (n=27) from the cold seep pockmark REGAB (5° 47.9'S, 9°42.7'E, 3170m
161 depth) in the Gulf of Guinea using the ROV Victor 6000 operated from the ship N/O
162 Pourquoi Pas? during the West African Cold Seeps (WACS) oceanographic cruise in January-
163 February 2011. Available physical and chemical characteristics for the sites: LS, MG and
164 REGAB are listed in Table 1. Mussels were collected in thermally insulated boxes containing
165 bottom seawater, brought on board by the ROV, and immediately placed in a cold room at
166 4°C. Gills, mantle and adductor muscle were then dissected and frozen in liquid nitrogen. An
167 additional piece of gill was sampled for FISH fixation in cold 4% paraformaldehyde in
168 filtered seawater and stored 4 hours at 4°C. Gills were then rinsed in filtered seawater and
169 dehydrated in graded ethanol concentrations. They were stored in absolute ethanol at 4°C for
170 transportation back to the laboratory. Mussel shells were measured for each sampled
171 individual. The shell lengths differed between the specimens from the two species: *B. aff.*
172 *boomerang* (50 to 160 mm) and *B. azoricus* (53-96 mm).

174 **2.2 Relative quantification of symbiont ratios and gene expression**

175 Genomic DNA from mussel and bacteria were extracted together from gill tissue using a
176 CTAB/PVP extraction procedure (2% CTAB, 1% PVP, 1.4 M NaCl, 0.2% beta-mercapto-
177 ethanol, 100 mM TrisHCl pH8, 0.1 mg.mL⁻¹ proteinase K, 1 mg.mL⁻¹ lysozyme). After
178 complete digestion of the tissues (1 h at 60°C), the mixture was incubated with 1 µl of RNase
179 for 30 min at 37°C. An equal volume of chloroform-isoamyl alcohol (24:1) was then added
180 and the tubes were slowly mixed by inversion for 3 min before a centrifugation at 14,000 rpm
181 at 4°C for 10 min. The supernatant was collected in a fresh tube, and DNA was precipitated
182 with 2/3 volume of cold isopropanol (1 h at -20°C). The DNA pellet was recovered by
183 centrifugation at 14,000 rpm at 4°C for 20 min, washed with 75% cold ethanol, air-dried and
184 re-suspended in 200 µl of sterile water. The relative ratio of symbionts in both mussel species
185 was estimated by real-time PCR amplification using 16S specific primers (Table 3) designed
186 according to the probes previously developed for FISH analysis (Duperron et al. 2006). All
187 experiments were carried out using a Chroma4 thermal cycler (Bio-Rad Laboratories, Inc.
188 Hercules, CA) and 1× ABsolute™QPCR SYBR® Green mix (ABgene, Epsom, UK), 70 nM
189 of each primer, and diluted DNA (2.5 ng in a final volume of 10 µl). A 120 bp-fragment of
190 cytosolic malate dehydrogenase gene (MDH) from the host was used as an internal PCR
191 control. The relative ratio of each symbiont type was estimated by the comparative Ct method
192 formula: $RQ = 2^{-\Delta Ct}$, with $\Delta Ct = Ct_{16S} - Ct_{MDH}$.

193 The expression of functional genes that are specific for a given metabolic pathway can be
194 considered as an appropriate tool for investigating the metabolic potential of an organism, and
195 can be an indicator of its physiological activity. In this study, we choose to analyze the
196 expression of two bacterial genes, the ATP-sulfurylase (specific of the SOX metabolism) and
197 the *pmoA* gene, which encodes for the particulate methane mono-oxygenase subunit-A
198 (specific of the MOX metabolism). Using gill tissue, total RNA for both mussels and bacteria
199 were extracted together using the Tri-Reagent (Invitrogen) according to the manufacturer's
200 instructions. Five μg of total RNA was reverse-transcribed using M-MLV reverse-
201 transcriptase (Promega, Madison, WI), random hexamers (Promega) and an anchor-oligo(dT)
202 primer (5'-CGCTCTAGAACTAGTGGATCT-3'). The relative gene expression of symbionts
203 in both mussel species was estimated by real time PCR amplification using specific ATP-
204 sulfurylase and *pmoA*-primers (Table 2; GenBank accession numbers AB178052 and
205 AY945761, respectively). A volume of 4 μl of each diluted reverse transcription product
206 (1:200 dilution) was subjected to real-time PCR in a final volume of 10 μl containing 70 nM
207 of primers and 1 \times ABsolute™ QPCR SYBR® Green Mix (ABgene). The amplification was
208 carried out as follows in triplicates: initial enzyme activation at 94°C for 15 min, then 40
209 cycles of 94°C for 15 sec, and then 60°C for 1 min. A fragment of ribosomal protein L15 gene
210 (RpL15) from the host was used as an internal PCR control (Table 3). Relative expression of
211 each gene was calculated according to the comparative Ct method using the formula: $RQ = 2^{-\Delta C_t}$
212 with $\Delta C_t = C_{tATPsulfur}$ or $C_{tpmoA} - C_{tRpL15}$.

2.3 Statistical Analysis

215 Data from quantitative real-time PCR experiments were tested for normality using the Shapiro
216 test, and differences in bacteria ratios and gene expression level were analyzed for
217 significance with a Welch t-test in the R Studio software (RStudio 0.96.122 Version, 2012).
218 Boston, <http://www.rstudio.org/>. Differences were considered statistically significant when
219 $p \leq 0.05$.

2.4 *In situ* hybridization (FISH)

222 Based on the results of SOX and MOX ratios, we chose 3 samples showing a high symbiont
223 ratio, and three samples showing a low symbiont ratio for each species previously fixed for
224 FISH. The gills embedded in paraffin were cut at 6 μm on a Leica, RM2245 microtome
225 (Germany). The sections were mounted on Super Frost slides (Euromedex, France) pre-coated

226 with Biobond (Euromedex, France). The slides were dewaxed and the gill tissue rehydrated in
227 a decreasing ethanol series. Hybridization was performed in a buffer composed of (0.18M
228 NaCl, 0.02 M Tris-HCl, 0.05 % SDS). To stain the symbionts, two probes were used: the
229 MOX-specific probe ImedM-138 (5'-ACCATGTTGTC CCCCCTAA-3') labeled with Cy3
230 (green), and the SOX-specific probe BangT-642 (5'-CCTATACTCTAGCTTGCCAG-3')
231 labeled with Cy5 (red) (Amann et al. 1990; Duperron et al. 2005, Duperron et al. 2008,
232 Duperron et al. 2011). The sections were incubated with 50 ng of each probe for hybridization
233 in a 30% formamide buffer, for 3 h at 46°C in pre-heated moisture chambers. After
234 hybridization, the samples were washed twice in a solution containing (0.04M NaCl, 0.04M
235 Tris/HCl, 0.1% SDS and 0.02M EDTA) at 48°C for 15 min, then rinsed with MilliQ water, air
236 dried, and mounted with VectaShield containing nuclear DAPI-staining and covered with a
237 coverslip sealed with nail-varnish. The hybridized sections were photographed under a
238 confocal laser-scanning microscope (Leica TCS SP5II, Germany).

240 3 Results

242 3.1 Relative quantification of symbiont ratios

243 The results show that the relative abundance of symbiont ratios and gene expression were
244 normally distributed for each sample tested in this study. The SOX and MOX ratios
245 determination in the two mussel species from the various sites at vents or at seeps are shown
246 in Fig. 1.

248 3.1.1 Variation in SOX

249 The Welch t-test showed no significant difference between SOX symbiont ratio quantified in
250 specimens from W01 (RQ = 312.0±41.7) compared to specimens from W02 and NW, (t=1.93,
251 p-value=0.059 and t=-0.8, p-value=0.40, respectively), but there was a significant difference
252 in SOX ratio between specimen from W02 and NW (t=-3.42, p-value=0.001). Mussels
253 collected at NW had a significantly higher SOX level (RQ = 355.6±32.7) compared to
254 mussels collected at W02 (RQ = 222.0±22.5) (Fig.1). No significant differences were detected
255 for SOX ratio between *B. azoricus* populations from the two vent sites, LS (RQ = 301.2±34.8)
256 and MG (RQ = 355.7±80.4) (t=-0.63, p-value=0.53) (Fig.1).

258 3.1.2 Variation in MOX ratio

1
2 259 Samples collected from the three REGAB sites exhibited similar MOX ratio (Fig. 1) with RQ
3
4 260 values at 384.1 ± 49.4 , 273.8 ± 37.4 and 301.3 ± 20.9 for NW, W01 and W02 respectively. These
5
6 261 relative quantities were comparable to those found for SOX ratio. No significant differences
7
8 262 were detected for MOX ratio between the two populations from LS (RQ = 38.2 ± 4.4) and MG
9
10 263 (RQ = 33.6 ± 3.8) ($t=0.82$, $p\text{-value}=0.42$) (Fig. 1) but these relative quantities were much lower
11
12 264 than those found for *B. azoricus* SOX ratio ($t=6.05$, $p\text{-value} = 1.358e-07$) (Fig. 1).
13

265

266 3.2 Relative quantification of symbiont gene expression

267 3.2.1 Variation in ATP sulfurylase gene expression

14
15
16 267
17
18 268 Using real-time PCR, no significant difference was detected ($t=0.53$ and $p\text{-value}=0.59$) in
19
20 269 symbiont-specific gene expression of ATP-sulfurylase between W01 and W02, but significant
21
22 270 differences were found between W01 and NW ($t=2.77$ and $p\text{-value}=0.01$), and between W02
23
24 271 and NW ($t=3.14$ and $p\text{-value}=0.003$). Mussels collected at NW had a lower ATP-sulfurylase
25
26 272 gene expression than the populations from W01 and W02 (Fig. 2). There was no significant
27
28 273 difference of symbiont gene expression of ATP-sulfurylase between the two vent fields MG
29
30 274 and LS ($t=-0.90$ and $p\text{-value}=0.36$) (Fig. 2).
31

275

32 276 3.2.2 Variation in pmoA gene expression

33
34 277 The *pmoA* gene encodes the active site of the pMMO (membrane-bound methane
35
36 278 monooxygenase) enzyme. The expression level of *pmoA* was generally very low in both
37
38 279 species (Fig. 2, note scale difference) with higher values for *B. azoricus* vs *B. aff. boomerang*.
39
40 280 Samples collected from the REGAB sites had similar levels of *pmoA* expression: 0.0011,
41
42 281 0.0035, and 0.162 at NW, W01, and W02 respectively (Fig. 2). No significant differences
43
44 282 were found in the expression of the symbiont-specific *pmoA* gene between the two vent fields
45
46 283 MG (RQ = 2.00) and LS (1.21) ($t=-1.53$ and $p\text{-value}=0.13$) (Fig. 2).
47

284

48 285 3.3 Comparative analysis of symbiont ratios and gene expression in two mussel species

49
50
51 286 A comparative analysis of symbiont ratios revealed similar SOX ratio ($t=-0.94$ and $p\text{-}$
52
53 287 $\text{value}=0.35$), but a significant difference in MOX ratio ($t=14.22$ and $p\text{-value}<2.2e^{-16}$) between
54
55 288 the two mussels species. The comparatively larger *B. aff. boomerang* species (shell length
56
57 289 between 50 and 160 cm) had markedly higher MOX ratio (316.24 ± 19.6) (Fig. 1), but lower
58
59 290 ATP-sulfurylase (3.04 ± 0.74) and *pmoA* (0.07 ± 0.05) gene expression, compared to the smaller
60
61 291 species *B. azoricus* (shell length between 53 and 96 cm), with values of (35.43 ± 2.8 , 46.42 ± 7.9)
62

292 and 1.69 ± 0.29 , for MOX ratio, ATP-sulfurylase and *pmoA* gene expression respectively (Fig.
293 2).

294

295 **3.4 FISH -In situ hybridization**

296 Fluorescence *in situ* hybridization of oligonucleotide probes to 16S RNA was used to identify
297 both MOX and SOX symbiont bacteria in gills of *Bathymodiolus* mussels (Fig. 3). MOX
298 dominated the gills of *B. aff. boomerang* and colonized the basal regions of the bacteriocytes
299 (Fig. 3 A, B), whereas they appeared faintly in *B. azoricus* (Fig. 3 C, D). In both
300 *Bathymodiolus* species, SOX were always found in the apical parts of the bacteriocytes and
301 were the most abundant symbiont in the gills of *B. azoricus* (Fig. 3 C, D). The evidence from
302 *in situ* hybridization shows that *B. aff. boomerang* from the deeper REGAB site had obviously
303 a greater symbiont ratio compared to *B. azoricus* (Fig. 3).

304

305 **4 Discussion:**

306 **4.1 Use of real time PCR to estimate symbiont ratios**

307 Relative or absolute quantification of symbiotic bacteria is necessary to understand the
308 dynamics of the symbiotic associations between chemoautotrophic bacteria (methanotrophs
309 and thiotrophs) and *Bathymodiolus* mussels. Previous microscopic studies have attempted to
310 quantify the relative abundance of each bacterial type (Salerno et al. 2005). Fiala-Médioni et
311 al (2002) qualitatively identified two symbiotic bacteria morphotypes in the gills of *B.*
312 *azoricus* and *B. heckerae* (a species living in cold seeps) using transmission electron
313 microscopy. Halary et al (2008) and Duperron et al (2011) used 3D-FISH to quantify the
314 volume occupied by different symbionts in bacteriocytes from *B. azoricus* and *B. aff.*
315 *boomerang*. The 3D-FISH technique is based on fluorescence *in situ* hybridization and image
316 analysis. The main limitation of microscopy techniques in quantification is the fact that they
317 do not estimate the total volume of symbionts in the entire gill of a specimen, but only in a
318 few thin section of this gill (Halary et al., 2008). Evidence for the activity of both sulfur-
319 oxidizing and methane-oxidizing metabolic pathways has also been reported in *B. azoricus*
320 (Fiala-Médioni et al. 2002). Regarding the stability of bacterial mRNA, a previous study
321 conducted on *B. puteoserpentis* (a vent species very close to *B. azoricus*) evidenced that the
322 half-life of *pmoA* mRNA was long, ranging from a few hours to several days (Wendeberg et
323 al. 2012). Deana and Belasco (2005) have shown that while bacterial mRNAs are actively

324 translated, they are very stable in comparison with their non-translated counterparts. In our
1 325 study, mussels are brought on board and dissected within 2 to 6 hours after sampling on the
2 326 bottom, optimizing the quality of mRNA. Indeed, using qPCR on DNA and RNA extracted
3 327 from a whole piece of gill, we are not able to take into account the local heterogeneity of the
4 328 symbiont distribution within each gill filament, but we generate a better estimation of the
5 329 relative ratio between both symbionts. In their study, Wendeberg et al (2012) localized *pmoA*
6 330 and *aprA* (encoding subunit A of the dissimilatory adenosine-5'-phosphosulfate-reductase
7 331 which is involved in the metabolism of the SOX symbiont). These authors evidenced gene
8 332 expression by FISH and showed that symbionts exhibited a stronger gene expression in
9 333 bacteriocytes close to the frontal ciliated surface at the posterior ends of the infra-branchial
10 334 chamber compared to the anterior gill ends. These authors also observed a high variability in
11 335 mRNA expression between samples that could reflect local modifications of the
12 336 environmental conditions.

337 In their study dedicated to the characterization of the SOX-symbiont population in the
338 bivalve *Codakia orbicularis*, Caro et al (2007) evidenced the existence of different sub-
339 populations characterized by various numbers of genome-copies ranging from haploid to
340 tetraploid stages. The multigenomic state of bacteria has been considered to be a signature of
341 their ability for rapid cell division when nutrients become available (Thorsen et al. 1992). The
342 ploidy degree has never been addressed in the symbiont of any *Bathymodiolus* species, so it is
343 at present impossible to know if one or both symbiont exhibit variable numbers of genome
344 copies and in which proportion. Our PCR approach does not allow to address this question
345 since we do not have any way to quantify the gill cells, nor the bacterial cells and then
346 subsequently establish a correlation between C(t) values and cell numbers. The observation of
347 polyploidy made by Caro et al (2007) could have an impact on what we have considered as
348 the symbiont ratio, in such a way that the real number of bacterial cells could not be directly
349 correlated with the C(t) value. Without any additional information, we assume that even this
350 could happen in mussel bacteriocytes, as the medium ratio of cells showing the different
351 polyploidy status is quite similar in all samples. Our ratios show differences between
352 individuals, even if not strictly correlated to an exact cell number. In previous studies using
353 FISH as a tool for symbiont ratios estimates, the question of the number of genome copies is
354 not addressed either although it might affect fluorescence intensity. Overall, FISH techniques
355 give a snapshot of a gill section, with precise and accurate spatial information but inadequate
356 quantitative estimates of relative abundance in symbiont ratio. Moreover FISH or TEM
357 techniques are time-consuming and only a limited number of samples/individuals can be

358 analyzed. Applying qPCR is considerably faster and cheaper, and allows taking into account a
359 large number of individuals and their natural variation. Therefore, the use of q-PCR approach
360 to estimate the relative abundance of symbionts in the mussel gills has to be considered as
361 complementary to other methods such as 2D or 3D FISH and TEM micrographs.
362 Furthermore, the expression of additional metabolic genes has to be considered to better
363 characterize the physiological status of symbionts. Genomes of both *B. azoricus* symbionts
364 genomes are presently being sequenced and annotated and this new information should help
365 resolve these problems.

367 **4.2 Variation in SOX ratio and ATP sulfurylase gene expression**

368 Mussels at the REGAB site were mostly concentrated in two areas: W01 and W02
369 (corresponding to M1 and M2 as described by Marcon et al. 2013). In our study, we focused
370 on mussels from three areas W01 and W02 described by Duperron et al (2005) and Olu-Leroy
371 et al (2007) and NW (NorthWest). We report the first data for symbiont ratios and gene
372 expression in *Bathymodiolus* specimens from the NW habitat.

373 The short distance that separate W02 from W01 (around 100 meters) may partly
374 explain the similar SOX ratio and ATP-sulfurylase expression in mussels from those areas,
375 and may also support the hypothesis that mussels from W01 and W02 are exposed to similar
376 environmental conditions. This is in agreement with previous studies conducted on mussels
377 from the REGAB site that showed no significant difference in SOX abundance in gills of *B.*
378 *aff. boomerang* collected in three areas separated by less than thirty meters (Duperron et al.
379 2011). The NW area is located 140 meters from W01 and at 190 meters from W02. Mussels
380 from NW seem to have a high SOX ratio and a low ATP-sulfurylase expression compared to
381 mussels from W02. These differences are likely the result of local differences in
382 environmental conditions specific to NW, as well as overall varying conditions at the REGAB
383 pockmark. Ondréas et al (2005), Charlou et al (2004) and Olu-Le Roy et al (2007) reported
384 that methane concentrations in the giant REGAB pockmark decrease from the center to the
385 periphery. Our results on the MOX and SOX symbionts in the mussels lead us to suggest that,
386 contrary to methane, sulfide concentrations increase in the center of REGAB pockmark
387 outward to the periphery. We also hypothesize that mussels from NW are exposed to more
388 transient sulfide fluxes than mussels from W02. According to Charlou et al (2004), the
389 methane concentration (13.85 $\mu\text{l/l}$) observed in an area close to NW was much lower than
390 those in W01 (89.51 $\mu\text{l/l}$) and W02 (128.9 $\mu\text{l/l}$). This may indicate that mussels from this area
391 rely more on sulfide than methane as an energy and carbon source to compensate for the

392 lower concentration of methane, Sulfide probably represents an important secondary energy
393 source for mussels from the NW. This implies that fluid flow is intense but different in the
394 three areas. The sulfide and methane concentrations were identified as important factors
395 influencing the symbiont bacteria quantities in gills of hydrothermal *Bathymodiolus* mussels
396 (Fiala- Médioni et al. 2002; Duperron et al. 2006), but the link between symbiont ratios and
397 environmental conditions is complex as evidenced by the fact that the SOX symbiont ratio is
398 similar in *B. azoricus* inhabiting two physically and chemically contrasting vent fields, LS and
399 MG. Our results suggest that the variation in sulfide availability in the cold seep areas
400 W01/W02 and NW impacted the SOX symbiont ratio in *B. aff. boomerang* at a short spatial
401 scale.

4.3 Variation in MOX ratio and pmoA gene expression

404 Mussels from W01, W02 and NW have statistically similar MOX ratio and pmoA expression
405 levels indicating that methane concentrations could be similar in these areas. The three
406 (smaller pockmark) sites sampled are located in the center of REGAB giant pockmark where
407 the methane flux is the highest and methane fluxes have been observed in all mussel beds
408 (Ondréas et al. 2005; Olu-Le Roy et al. 2007; Marcon et al. 2013). MOX ratio and pmoA
409 expression were also similar for *B. azoricus* specimens from two hydrothermal sites, LS and
410 MG. We have no specific measurements of sulfide and methane in the vicinity of the *B.*
411 *azoricus* mussel beds sampled, but as previously reported, reduced concentrations of sulfide
412 were measured in fluids at MG ranging from 0.6 to 3.3 mM, and at LS from 1.3 to 1.82 mM
413 while methane concentrations of up to 0.52 mM and 1.7 μ M were measured at LS and MG
414 respectively (Douville et al. 2002; Charlou et al. 2002, Chiralou et al. 2004). These findings
415 are in agreement with our results and could explain the predominance of SOX thiotrophic
416 symbionts in the gills of all specimens of *B. azoricus*.

4.4 Comparative analysis of symbiont ratios and gene expression between species

419 In the present study, we report the first attempt to compare symbiont ratios and gene
420 expression in the gills of two *Bathymodiolus* species from contrasting environments:
421 hydrothermal vents and cold seeps. Our results indicate that the MOX ratio is higher in the
422 gills of *B. aff. boomerang* compared to *B. azoricus*. The dominance of MOX is not surprising
423 since methane concentrations are significantly higher in cold seeps. Mussel beds from the
424 three areas within REGAB pockmark showed obvious pulses of free methane gas into the
425 water column, which could result in an appreciable variability in the concentration of gas

426 (Boetius and Suess 2004; De Beer et al. 2006; Niemann et al. 2006). These observations
1 427 support the hypothesis that relative abundance of symbiont bacteria could be significantly
2 428 influenced by environmental conditions (Fiala- Médioni et al. 2002; Duperron et al. 2006).
3 429 The average ratio and gene expression for each symbiont was significantly different between
4 430 species. *B. aff. boomerang* from deeper sites (3170 m) exhibits a higher symbiont ratio, but
5 431 associated with the lowest gene expression. Generally, mussels collected from shallow water
6 432 benefit from a higher particulate flux (Riou et al. 2010) which is the case for MG and LS
7 433 populations that are located at 830 and 1700 meters depth respectively. The presence of
8 434 particle flux suggests that these mussels could rely less on symbionts to meet their carbon
9 435 needs. At the contrary, in the deeper sites, particles are less accessible to mussels increasing
10 436 the dependence of mussels on their symbionts. Surprisingly, we observed that gene expression
11 437 of both ATP-sulfurylase and *pmoA* are significantly higher in *B. azoricus* individuals
12 438 suggesting that gene expression in both species can be modulated by various factors, but also
13 439 that there is no evident correlation between symbiont ratios and gene expression at least for
14 440 these metabolisms. Evidence from *in situ* hybridization experiments confirm that symbiont
15 441 bacteria are abundantly expressed in gills of *B. aff. boomerang*. In contrast, less symbiont
16 442 bacteria were detected in *B. azoricus*. Our qPCR and FISH results are congruent on this aspect
17 443 and both indicate that chemosynthetic bacteria make a substantial contribution to the nutrition
18 444 of the *B. aff. boomerang*.

19 445 For both species, size dependent variations on symbiont ratios and gene expression
20 446 were not significant as found by Duperron et al (2011). Martins et al (2008) showed that small
21 447 individuals of *B. azoricus* mussels were strongly dependent on filter-feeding while larger
22 448 mussels obtained a significant portion of their energy from endosymbiosis, suggesting that
23 449 symbiont ratios could increase with age. We did not observe such correlation between
24 450 symbiont ratios and mussel size in our *B. azoricus* sample but this might be due to the fact
25 451 that very small specimens were not present in our collection.

26 452 To conclude, we have presented a comparative analysis of symbiont ratios and gene
27 453 expression in the gills of two *Bathymodiolus* species to improve the understanding of inter-
28 454 and intra-site variability observed in mussels from contrasting environments. Symbiont ratios
29 455 in the gills of mussels reflect the environmental levels of methane and sulfide. *B. aff.*
30 456 *boomerang* from a methane rich environment (cold seeps) showed a significantly higher
31 457 relative abundance of MOX, and *B. azoricus* from a sulfide rich environment (hydrothermal
32 458 vent) showed a significantly higher relative abundance of SOX. We also evidenced that
33 459 symbiont ratios (based on 16S DNA qPCR assay) is not strictly correlated to gene expression

460 for ATP-sulfurylase and pmoA (based on mRNA qPCR assay). A complementary work based
1
2 461 on the use of more genes from metabolic pathways has to be performed to further explore this
3
4 462 relation.

5 463

6
7 464

8
9
10
11
12
13
14
15
16
17
18
19
20
21
22
23
24
25
26
27
28
29
30
31
32
33
34
35
36
37
38
39
40
41
42
43
44
45
46
47
48
49
50
51
52
53
54
55
56
57
58
59
60
61
62
63
64
65

465 **Acknowledgements**

1
2 466 We thank the crew and pilots of the NO Pourquoi Pas? and the ROV Victor 6000 for their
3
4 467 assistance and technical support, as well as the chief scientist Dr. Karine Olu Le Roy during
5
6 468 the cruise WACS (2011) and Dr. François Lallier, during the cruise BIOBAZ (2011). We
7
8 469 thank Dr. Sophie Le Panse, manager of Optical Imaging Platform Merimage of the Station
9
10 470 Biologique de Roscoff, for having introduced us (HG and AA) to the confocal microscopy.
11
12 471 This work was funded by the Région Bretagne with the help of GIS Europole Mer (HG), and
13 472 the JST/CNRS *Bathymodiolus* program (AT, FHL).
14
15
16 473
17
18 474
19
20

21 475 **References**

- 22
23
24 476 Amann R, Binder BJ, Olson RJ, Chisholm SW, Devereux R, Stahl DA (1990) Combination of
25
26 477 16S rRNA-targeted oligonucleotide probes with flow cytometry for analyzing mixed
27
28 478 microbial populations. *Appl Environ Microbiol* 56:1919–1925
29
30 479 Barry JP, Buck KR, Kochevar RK, Nelson DC, Fujiwara Y, Goffredi SK, Hashimoto J (2002)
31 480 Methane-based symbiosis in a mussel, *Bathymodiolus platifrons*, from cold seeps in
32
33 481 Sagami Bay, Japan. *Invert Biol* 121:47–54
34
35 482 Boetius A, Suess E (2004) Hydrate Ridge: a natural laboratory for the study of microbial life
36
37 483 fueled by methane from near-surface gas hydrates. *Chemical Geology* 205:291–310
38
39 484 Boutet I, Ripp R, Lecompte O, Dossat C, Corre E, Tanguy A, Lallier F (2011) Conjugating
40 485 effects of symbionts and environmental factors on gene expression in deep-sea
41
42 486 hydrothermal vent mussels. *BMC genomics* 12:530
43
44 487 Caro A, Gros O, Got P, De Wit R, Troussellier M (2007) Characterization of the Population
45
46 488 of the Sulfur-Oxidizing Symbiont of *Codakia orbicularis* (Bivalvia, Lucinidae) by
47
48 489 Single-Cell Analyses. *Appl Environ Microbiol* 73: 2101–2109
49
50 490 Cavanaugh CM (1983) Symbiotic chemoautotrophic bacteria in marine invertebrates from
51
52 491 sulfide-rich habitats. *Nature* 302:58–61
53
54 492 Cavanaugh CM, McKiness ZP, Newton ILG, Stewart FJ (2006) Marine Chemosynthetic
55 493 Symbioses. In: Dworkin M., Falkow S., Rosenberg E., Schleifer K.-H., Stackebrandt
56
57 494 E. (eds) *The Prokaryotes*. Springer New York, New York, NY, pp 475–507
58
59 495 Charlou JL, Donval JP, Fouquet Y, Jean-Baptiste P, Holm N (2002) Geochemistry of high H₂
60
61
62
63
64
65

496 and CH₄ vent fluids issuing from ultramafic rocks at the Rainbow hydrothermal field
1 497 (36°14' N, MAR). Chem Geol 191:345–359
2
3 498 Charlou JL, Donval J, Fouquet Y, Ondreas H, Knoery J, Cochonat P, Levaché D, Poirier Y,
4
5 499 Jean-Baptiste P, Fourré E, Chazallon B (2004) Physical and chemical characterization
6
7 500 of gas hydrates and associated methane plumes in the Congo–Angola Basin. Chem
8
9 501 Geol 205:405–425
10
11 502 Childress JJ, Fisher CR, Brooks JM, Kennicutt MC, Bidigare R, Anderson AE (1986) A
12
13 503 Methanotrophic Marine Molluscan (Bivalvia, Mytilidae) Symbiosis: Mussels Fueled
14
15 504 by Gas. Science 233:1306–1308
16
17 505 Childress JJ, Fisher CR, Favuzzi JA, Kochevar RE, Sanders NK, Alayse AM (1991) Sulfide-
18
19 506 driven autotrophic balance in the bacterial symbiont-containing hydrothermal vent
20
21 507 tubeworm, *Riftia pachytila* Jones. Biol Bull 180:135–153
22
23 508 De Beer D, Sauter EJ, Niemann H, Kaul N, Foucher J-P, Witte U, Schlüter M, Boetius A
24
25 509 (2006) In situ fluxes and zonation of microbial activity in surface sediments of the
26
27 510 Haakon Mosby Mud Volcano. Lim Oceano 51: 1315-1331
28
29 511 DeChaine EG, Bates AE, Shank TM, Cavanaugh CM (2006) Off-axis symbiosis found:
30
31 512 characterization and biogeography of bacterial symbionts of Bathymodiolus mussels
32
33 513 from Lost City hydrothermal vents. Environ Microbiol 8:1902–1912
34
35 514 DeChaine EG, Cavanaugh CM (2006) Symbioses of methanotrophs and deep-sea mussels
36
37 515 (Mytilidae: Bathymodiolinae). Molecular basis of symbiosis. Springer, pp 227–249
38
39 516 Desbruyères D, Biscoito M, Caprais J-C, Colaço A, Comtet T, Crassous P, Fouquet Y,
40
41 517 Khripounoff A, Le Bris N, Olu K, Riso R, Sarradin P-M, Segonzac M, Vangriesheim
42
43 518 A (2001) Variations in deep-sea hydrothermal vent communities on the Mid-Atlantic
44
45 519 Ridge near the Azores plateau. Deep Sea Research Part I: Oceano Res Papers
46
47 520 48:1325–1346
48
49 521 Dickens GR (2003) Rethinking the global carbon cycle with a large, dynamic and microbially
50
51 522 mediated gas hydrate capacitor. Earth Plan Sci Letters 213:169–183
52
53 523 Distel DL, Lee HK, Cavanaugh CM (1995) Intracellular coexistence of methano- and thio-
54
55 524 autotrophic bacteria in a hydrothermal vent mussel. Proc Natl Acad Sci 92:9598–9602
56
57 525 Douville E, Charlou J, Oelkers E, Bienvenu P, Jove Colon C, Donval J, Fouquet Y, Prieur D,
58
59 526 Appriou P (2002) The rainbow vent fluids (36°14'N, MAR): the influence of
60
61 527 ultramafic rocks and phase separation on trace metal content in Mid-Atlantic Ridge
62
63 528 hydrothermal fluids. Chem Geol 184:37–48
64
65 529 Dubilier N, Bergin C, Lott C (2008) Symbiotic diversity in marine animals: the art of

530 harnessing chemosynthesis. Nat Rev Microbiol 6:725–740

1
2 531 Duperron S, Nadalig T, Caprais J-C, Sibuet M, Fiala-Medioni A, Amann R, Dubilier N

3 532 (2005) Dual Symbiosis in a *Bathymodiolus* sp. Mussel from a Methane Seep on the

4
5 533 Gabon Continental Margin (Southeast Atlantic): 16S rRNA Phylogeny and

6
7 534 Distribution of the Symbionts in Gills. Appl Env Microbiol 71:1694–1700.

8
9 535 Duperron S, Bergin C, Zielinski F, Blazejak A, Pernthaler A, McKiness ZP, DeChaine E,

10
11 536 Cavanaugh CM, Dubilier N (2006) A dual symbiosis shared by two mussel species,

12
13 537 *Bathymodiolus azoricus* and *Bathymodiolus puteoserpentis* (Bivalvia: Mytilidae),

14
15 538 from hydrothermal vents along the northern Mid-Atlantic Ridge. Environ Microbiol

16
17 539 8:1441–1447

18 540 Duperron S, Fiala-Médioni A, Caprais JC, Olu K, Sibuet M (2007) Evidence for

19
20 541 chemoautotrophic symbiosis in a Mediterranean cold seep clam (Bivalvia: Lucinidae):

21
22 542 comparative sequence analysis of bacterial 16S rRNA, APS reductase and RubisCO

23
24 543 genes: Symbiosis in a cold-seep lucinid. FEMS Microbiol Ecol 59:64–70

25
26 544 Duperron S, Halary S, Lorion J, Sibuet M, Gaill F (2008) Unexpected co-occurrence of six

27
28 545 bacterial symbionts in the gills of the cold seep mussel *Idas* sp. (Bivalvia: Mytilidae).

29
30 546 Environ Microbiol 10:433–445

31 547 Duperron S, Guezi H, Gaudron SM, Pop Ristova P, Wenzhöfer F, Boetius A (2011) Relative

32
33 548 abundances of methane- and sulphur-oxidising symbionts in the gills of a cold seep

34
35 549 mussel and link to their potential energy sources. Geobiology 9:481–491

36
37 550 Felbeck H, Childress JJ, Somero GN (1981) Calvin-Benson cycle and sulfide oxidation

38
39 551 enzymes in animals from sulfide-rich habitats. Nature 293:291–293

40 552 Fiala-Médioni A, McKiness Z, Dando P, Boulegue J, Mariotti A, Alayse-Danet A, Robinson

41
42 553 J, Cavanaugh C (2002) Ultrastructural, biochemical, and immunological

43
44 554 characterization of two populations of the mytilid mussel *Bathymodiolus azoricus*

45
46 555 from the Mid-Atlantic Ridge: evidence for a dual symbiosis. Mar Biol 141:1035–1043

47
48 556 Fisher CR, Childress JJ, Oremland RS, Bidigare RR (1987) The importance of methane and

49
50 557 thiosulfate in the metabolism of the bacterial symbionts of two deep-sea mussels. Mar

51
52 558 Biol 96:59–71

53 559 Fisher CR, Brooks JM, Vodenichar JS, Zande JM, Childress JJ (1993) The Co-occurrence of

54
55 560 Methanotrophic and Chemoautotrophic Sulfur-Oxidizing Bacterial Symbionts in a

56
57 561 Deep-sea Mussel. Mar Ecol 14:277–289

58
59 562 Fujiwara Y, Takai K, Uematsu K, Tsuchida S, Hunt JC, Hashimoto J (2000) Phylogenetic

60
61 563 characterization of endosymbionts in three hydrothermal vent mussels: influence on

- 564 host distributions. *Mar Ecol Prog Ser* 208:147–155
- 1
2 565 Génio L, Johnson SB, Vrijenhoek RC, Cunha MR, Tyler PA, Kiel S, Little CT (2008) New
3
4 566 record of “*Bathymodiolus*” *mauritanicus* Cosel 2002 from the Gulf of Cadiz (NE
5
6 567 Atlantic) mud volcanoes. *J Shellfish Res* 27:53–61
- 7 568 Geret F, Rouse N, Riso R, Sarradin PM, Cosson RP (1998) Metal compartmentalization and
8
9 569 metallothionein isoforms in mussels from the Mid-Atlantic Ridge; preliminary
10
11 570 approach to the fluid-organism relationship. *Cah Biol Mar* 39(3-4): 291-293
- 12
13 571 Geret F, Riso R, Sarradin PM, Caprais JC, Cosson RP (2002). Metal bioaccumulation and
14
15 572 storage forms in the shrimp, *Rimicaris exoculata*, from the Rainbow hydrothermal
16
17 573 field (Mid-Atlantic Ridge); preliminary approach to the fluid–organism relationship.
18
19 574 *Cah Biol Mar* 43, 43– 52
- 20 575 German CR, Lin J (2004) The thermal structure of the oceanic crust, ridge-spreading and
21
22 576 hydrothermal circulation: How well do we understand their inter-connections? In:
23
24 577 German C.R., Lin J., Parson L.M. (eds) *Geophysical Monograph Series*. American
25
26 578 *Geophysical Union*, Washington, D. C., pp 1–18
- 27 579 Gibson RN, Atkinson RJA, Gordon JDM (2005) Ecology of cold seep sediments: interactions
28
29 580 of fauna with flow, chemistry and microbes. *Oceano Mar Biol Annu Rev* 43:1–46
- 30
31 581 Girguis PR (2006) Metabolite uptake, stoichiometry and chemoautotrophic function of the
32
33 582 hydrothermal vent tubeworm *Riftia pachyptila*: responses to environmental variations
34
35 583 in substrate concentrations and temperature. *J Exp Biol* 209:3516–3528
- 36 584 Girguis PR, Childress JJ (2006). Metabolite stoichiometry and chemoautotrophic function of
37
38 585 the hydrothermal vent tubeworm *Riftia pachyptila*: responses to environmental
39
40 586 variations in substrate concentrations and temperature. *J. Exp. Biol.* 209: 3516–3528
- 41
42 587 Halary S, Riou V, Gaill F, Boudier T, Duperron S (2008) 3D FISH for the quantification of
43
44 588 methane- and sulphur-oxidizing endosymbionts in bacteriocytes of the hydrothermal
45
46 589 vent mussel *Bathymodiolus azoricus*. *The ISME Journal* 2:284–292
- 47 590 Helmstetter CE, Cooper S (1968) DNA synthesis during the division cycle of rapidly growing
48
49 591 *E. coli* B/r. *J Mol Biol* 31:507–518
- 50
51 592 Kádár E, Bettencourt R, Costa V, Santos RS, Lobo-da-Cunha A, Dando P (2005)
52
53 593 Experimentally induced endosymbiont loss and re-acquirement in the hydrothermal
54
55 594 vent bivalve *Bathymodiolus azoricus*. *J Exp Mar Biol Ecol* 318:99–110
- 56 595 Kenk VC, Wilson BR (1985) A new mussel (*Bivalvia*, *Mytilidae*) from hydrothermal vents in
57
58 596 the Galapagos Rift zone. *Malacologia* 26:253–271
- 59
60 597 Kojima S (2002) Deep-sea chemoautosynthesis-based communities in the northwestern
61
62
63
64
65

598 Pacific. J Oceano 58: 343-363

1
2 599 Le Bris N, Sarradin PM, Caprais JC (2003) Contrasted sulphide chemistries in the
3
4 600 environment of 13°N EPR vent fauna. Deep Sea Research Part I: Oceano Res Papers
5 601 50:737–747
6

7 602 Le Pennec M, Diouris M, Herry A (1988) Endocytosis and lysis of bacteria in gill
8
9 603 epithelium of *Bathymodiolus thermophilus*, *Thyasira flexuosa* and *Lucinella*
10 604 *divaricata* (Bivalve, Molluscs). J Shellfish Res 7: 483-489
11

12 605 Levin LA (2005). Ecology of cold seep sediments: interactions of fauna with flow, chemistry,
13
14 606 and microbes. Oceanogr. Mar. Biol. Ann Rev 43, 1–46.
15

16 607 Lewis KB, Marshall BA (1996). Seep faunas and the other indicators of methane-rich
17
18 608 dewatering on New Zealand convergent margins. New Zealand J. of Geol Geophy
19
20 609 39, 181–200
21

22 610 Levin LA, Dayton PK (2009) Ecological theory and continental margins: where shallow
23
24 611 meets deep. Trends Ecol Evol 24:606–617
25

26 612 Lonsdale P, Becker K (1985) Hydrothermal plumes, hot springs, and conductive heat flow in
27
28 613 the Southern Trough of Guaymas Basin. Earth Plan Sci Letters 73:211–225
29

30 614 MacDonald IR, Boland GS, Baker JS, Brooks JM, Kennicutt II MC, Bidigare RR (1989) Gulf
31
32 615 of Mexico hydrocarbon seep communities. Mar Biol 101:235–247
33

34 616 Marcon Y, Sahling H, Allais AG, Bohrmann G, Olu K (2013) Distribution and temporal
35
36 617 variation of mega-fauna at the Regab pockmark (Northern Congo Fan), based on a
37
38 618 comparison of videomosaics and geographic information systems analyses. Mar Ecol.
39
40 619 SSN 0173-9565: 1-19.doi: 10.1111/maec.12056
41

42 620 Martins I, Colaço A, Dando PR, Martins I, Desbruyères D, Sarradin P-M, Marques JC,
43
44 621 Serrão-Santos R (2008) Size-dependent variations on the nutritional pathway of
45
46 622 *Bathymodiolus azoricus* demonstrated by a C-flux model. Ecol Model 217:59–71
47

48 623 Nelson DC, Fisher CR (1995) Chemoautotrophic and methanotrophic endosymbiotic bacteria
49
50 624 at deep-sea vents and seeps. In Microbiology of deep-sea hydrothermal vents Karl DM
51
52 625 (ed) Boca Raton FL:CRC Press inc pp 125-167
53

54 626 Nelson DC, Hagen KD, Edwards DB (1995) The gill symbiont of the hydrothermal vent
55
56 627 mussel *Bathymodiolus thermophilus* is a psychrophilic, chemoautotrophic, sulfur
57
58 628 bacterium. Mar Biol 121:487–495
59

60 629 Niemann H, Lösekann T, de Beer D, Elvert M, Nadalig T, Knittel K, Amann R, Sauter EJ,
61
62 630 Schlüter M, Klages M, Foucher JP, Boetius A (2006) Novel microbial communities of
63
64 631 the Haakon Mosby mud volcano and their role as a methane sink. Nature 443:854–858
65

- 632 Olu-Le Roy K, Caprais J-C, Fifis A, Fabri M-C, Galéron J, Budzinsky H, Le Ménach K,
1 633 Khripounoff A, ééas H, Sibuet M (2007) Cold-seep assemblages on a giant pockmark
2
3 634 off West Africa: spatial patterns and environmental control. *Mar Ecol* 28:115–130
4
5 635 Ondréas H, Olu K, Fouquet Y, Charlou JL, Gay A, Dennielou B, Donval JP, Fifis A, Nadalig
6
7 636 T, Cochonat P, Cauquil E, Bourillet JF, Moigne ML, Sibuet M (2005) ROV study of a
8
9 637 giant pockmark on the Gabon continental margin. *Geo Mar Letters* 25:281–292
10
11 638 Pimenov NV, Kalyuzhnaya MG, Khmelenina VN, Mityushina LL, Trotsenko YA (2002)
12
13 639 Utilization of methane and carbon dioxide by symbiotrophic bacteria in gills of
14
15 640 Mytilidae (*Bathymodiolus*) from the Rainbow and Logachev hydrothermal fields on
16
17 641 the Mid-Atlantic Ridge. *Microbiology* 71:587–594
18
19 642 Riou V, Duperron S, Halary S, Dehairs F, Bouillon S, Martins I, Colaço A, Serrão Santos R
20
21 643 (2010) Variation in physiological indicators in *Bathymodiolus azoricus* (Bivalvia:
22
23 644 Mytilidae) at the Menez Gwen Mid-Atlantic Ridge deep-sea hydrothermal vent site
24
25 645 within a year. *Mar Environ Res* 70:264–271
26
27 646 Robinson JJ, Polz MF, Fiala-Medioni A, Cavanaugh CM (1998) Physiological and
28
29 647 immunological evidence for two distinct C1-utilizing pathways in *Bathymodiolus*
30
31 648 *puteoserpentis* (Bivalvia: Mytilidae), a dual endosymbiotic mussel from the Mid-
32
33 649 Atlantic Ridge. *Mar Biol* 132:625–633
34
35 650 Salerno JL, Macko SA, Hallam SJ, Bright M, Won Y-J, McKiness Z, Van Dover CL (2005)
36
37 651 Characterization of symbiont populations in life-history stages of mussels from
38
39 652 chemosynthetic environments. *Biol Bull* 208:145–155
40
41 653 Sibuet M, Olu K (1998) Biogeography, biodiversity and fluid dependence of deep-sea cold-
42
43 654 seep communities at active and passive margins. *Deep-Sea Research Part II* 45:517–
44
45 655 567
46
47 656 Tivey MK (1995). Modeling chimney growth and associated fluid flow at seafloor
48
49 657 hydrothermal vent sites. In Humphris SE, Zierenberg RA, Mullineaux LS, and
50
51 658 Thomson RE. (Eds.), *Seafloor Hydrothermal Systems: Physical, Chemical, Biol Geol*
52
53 659 *Interac*, Am.Geophys. Union, Geophys. Monogr., 91:158-177
54
55 660 Thorsen BK, Enger O, Norland S. Hoff KJ. (1992) Long-term starvation survival of *Yersinia*
56
57 661 *ruckeri* at different salinities studied by microscopical and flow cytometric methods.
58
59 662 *Appl. Environ Microbiol.* 58:1624–1628
60
61 663 Van Dover CL (2000) *The ecology of deep-sea hydrothermal vents*. Princeton University
62
63 664 Press, Princeton, N.J
64
65

- 665 Van Dover CL, Trask JL (2000) Diversity at deep-sea hydrothermal vent and intertidal mussel
666 beds. *Mar Ecol Prog Ser* 195:169–178
- 667 Van Dover CL (2002) Evolution and Biogeography of Deep-Sea Vent and Seep Invertebrates.
668 *Science* 295:1253–1257
- 669 Van Dover CL, Aharon P, Bernhard JM, Caylor E, Doerries M, Flickinger W, Gilhooly W,
670 Goffredi SK, Knick KE, Macko SA, Rapoport S, Raulfs EC, Ruppel C, Salerno JL,
671 Seitz RD, Sen Gupta BK, Shank T, Turnipseed M, Vrijenhoek R (2003) Blake Ridge
672 methane seeps: characterization of a soft-sediment, chemosynthetically based
673 ecosystem. *Deep Sea Research Part I: Oceano Res Papers* 50:281–300
- 674 Vanreusel A, Fonseca G, Danovaro R, Da Silva MC, Esteves AM, Ferrero T, Gad G,
675 Galtsova V, Gambi C, Da Fonsêca Genevois V, Ingels J, Ingole B, Lampadariou N,
676 Merckx B, Miljutin D, Miljutina M, Muthumbi A, Netto S, Portnova D, Radziejewska
677 T, Raes M, Tchesunov A, Vanaverbeke J, Van Gaever S, Venekey V, Bezerra TN,
678 Flint H, Copley J, Pape E, Zeppilli D, Martinez PA, Galeron J (2010) The contribution
679 of deep-sea macrohabitat heterogeneity to global nematode diversity: Nematode
680 diversity and habitat heterogeneity. *Mar Ecol* 31:6–20
- 681 Von Damm KL (1995) Controls on the chemistry and temporal variability of seafloor
682 hydrothermal fluids. In: Humphris SE, Zierenberg RA, Mullineaux LS, Thomson RE
683 (eds) *Geophysical Monograph Series*. American Geophysical Union, Washington, D.
684 C., pp 222–247
- 685 Won YJ, Hallam SJ, O'Mullan GD, Pan IL, Buck KR, Vrijenhoek RC (2003) Environmental
686 Acquisition of Thiotrophic Endosymbionts by Deep-Sea Mussels of the Genus
687 *Bathymodiolus*. *Appl Environ Microbiol* 69:6785–6792

TABLES

Table1: Sulfide and methane concentrations recorded in fluids at Menez Gwen and Lucky Strike. (adapted from Douville et al. 2002; Charlou et al. 2000, 2004) and methane concentration reported around mussels at three minor pockmarks within REGAB giant pockmark (Charlou et al. 2004). ND: not determined.

SITES	DEPTH (m)	H ₂ S concentration	CH ₄ concentration
LS	1700	0.6-3.3 (mM)	0.52 (mM)
MG	850	1.3-1.82 (mM)	1.7 (mM)
W01	3156	ND	89.5 µl/l
W02	3156	ND	128.9 µl/l
NW	3156	ND	13.8 µl/l

Table 2: Primers used in real-time PCR amplification of bacteria and host gene.

Genes	Primer sequence 5'-3'
Sulfide oxidizer symbiont 16S(SOX)	115F : 5'-GAGTAACGCGTAGGAATCTGC-3' 193R : 5'-CGAAGGTCTCCACTTTACTCCATAGAG-3'
Methanotrophic symbiont 16S (MOX)	515F: 5'-GTGCCAGCMGCCGCGGTAA-3' 845R: 5'-GCTCCGCCACTAAGCCTATAAATAGACC-3'
Cytosolic malate dehydrogenase (host) (MDH)	For: 5'- ATGGAGGAAAAGAGATATGGCACTGAGCGT-3' Rev: 5'-TAACATTAACATAGCCTAGGAACCTAATG-3'
ATP sulfurylase	For: 5'- GTGCGTGATGCCGCTATCCGCACCATG-3' Rev : 5'-GGTCCGGCATAGAGCATGTCAAACGGATA-3'
particulate methanemethanomonooxygenase subunit A (PMOA)	For : 5'-GAGTGGATTAACAGATATTTGAACTTCTGG-3' Rev : 5'-CATACCACCAACAACAGCTGTAAGTACAAA-3'
ribosomal protein L15 gene (RPL15)	For 5'-TATGGTAAACCTAAGACACAAGGAGT-3' Rev 5'-TGGAATGGATCAATCAAAATGATTTC-3'

FIGURES

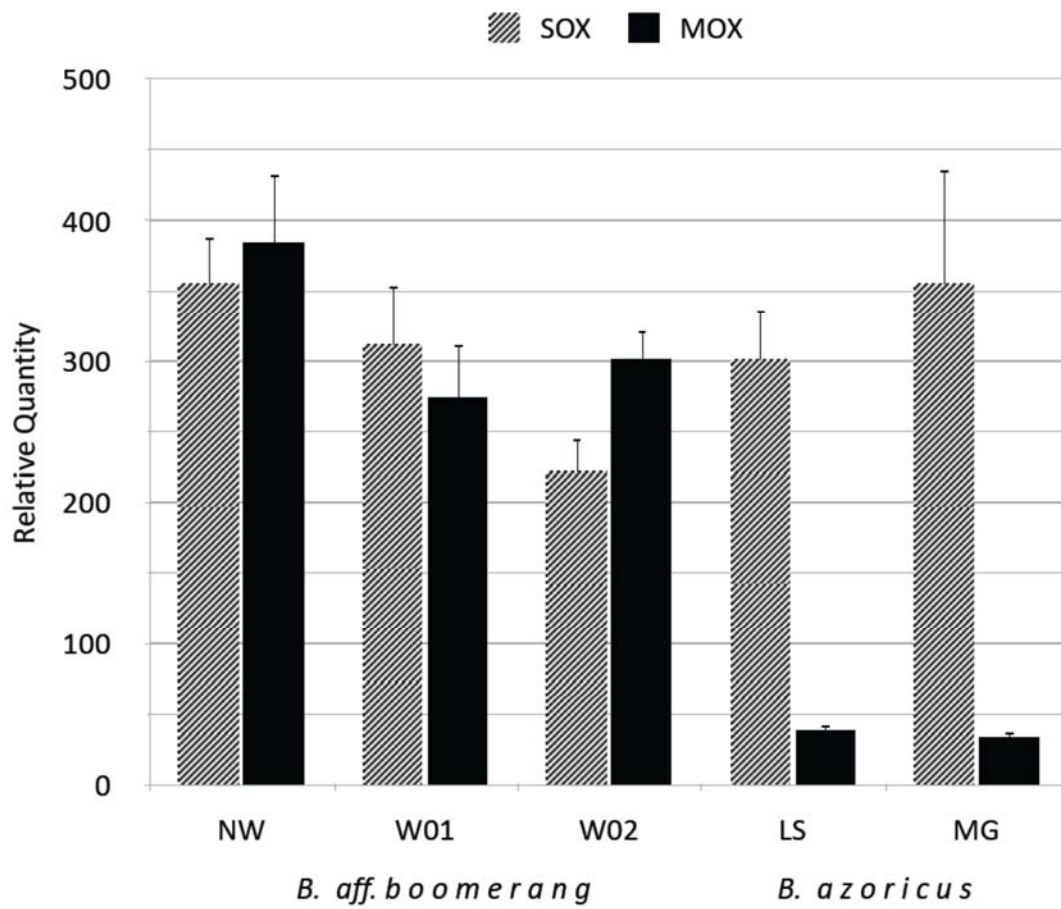


Fig. 1 Relative quantification of thiotrophic symbiont (SOX) and methanotrophic symbiont (MOX) in gills of *B. aff. boomerang* collected from three sampling areas, W01 (n= 28), W02 (n=43) and NW (n=27) and *B. azoricus* collected from two vent fields, MG (n=33) and LS (n=22).

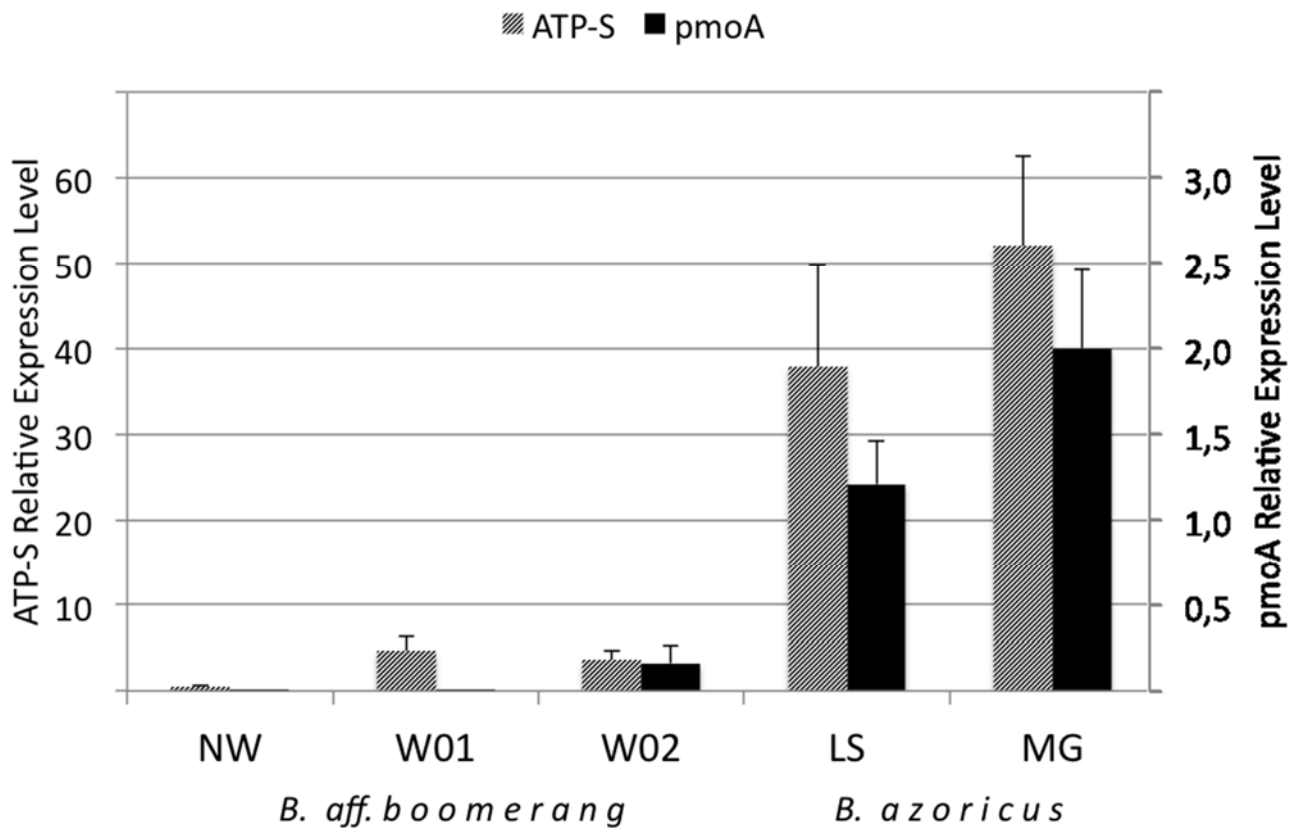


Fig. 2 Relative quantification of ATP sulfurylase (ATP-S) and particulate methane oxygenase, subunit A (pmoA) gene expression in gills of *B. aff. boomerang* collected from three cold seep sampling areas, W01 (n=28), W02 (n=43) and NW (n=27), and *B. azoricus* collected from two vent fields, MG (n=33) and LS (n=22).

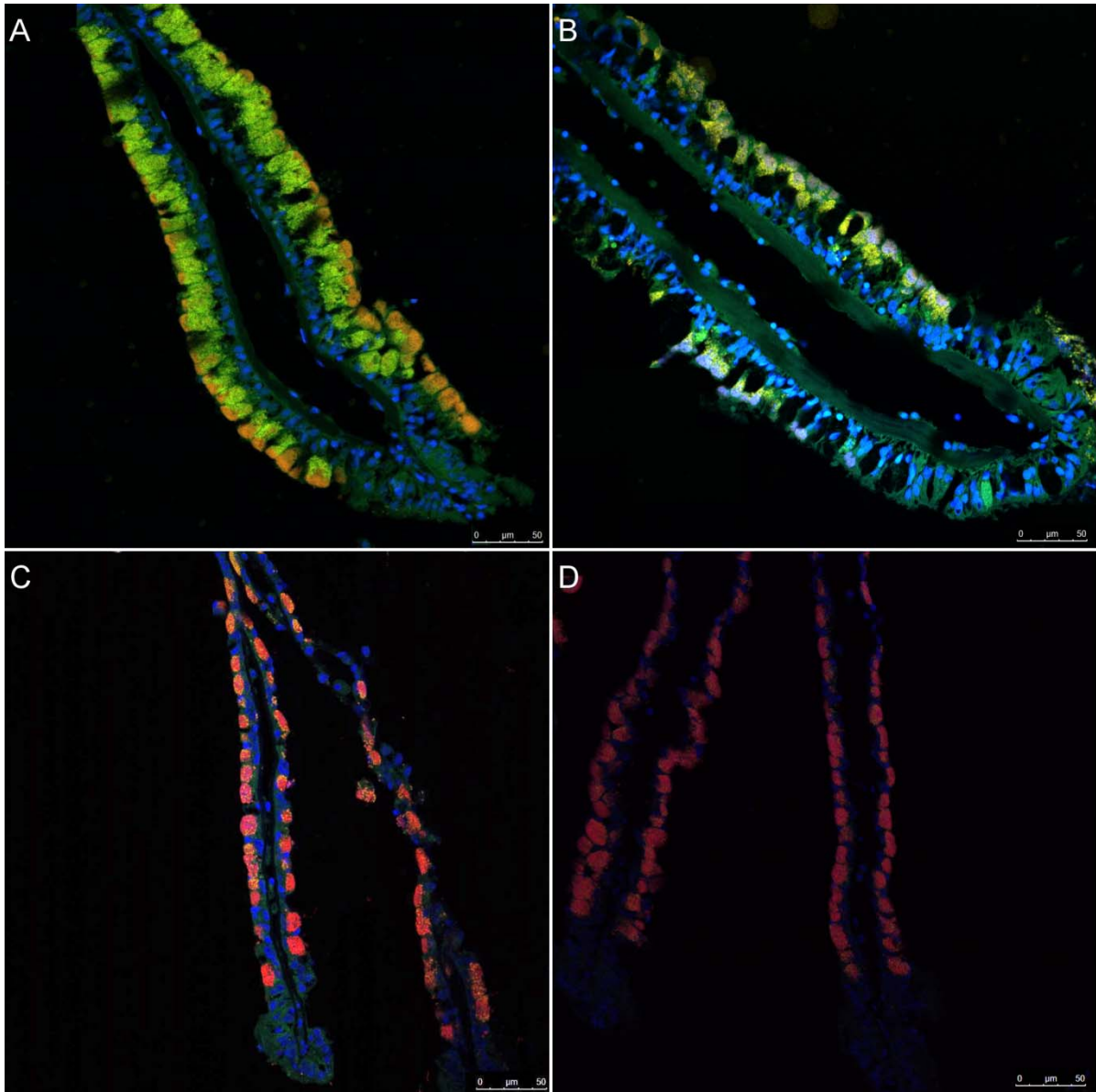


Fig. 3 Localization of MOX (green, FISH probeImedM-138) and SOX (orange, FISH probeBangT193) symbionts in gill cross-sections from *B. aff. boomerang* with high (A), and low (B) MOX symbiont content and from *B. azoricus* with high (C) and low (D) SOX symbiont content. Host cell nuclei are blue (DAPI).